



## Electric and Dielectric Studies on Modified Lithium Germanate

Jaimon C Johnson<sup>a</sup>, Parvez J Qureshi<sup>a</sup>, Ishakapte<sup>a</sup>, Sucharita Niyogi<sup>a</sup> & Madhuri W<sup>b\*</sup>

<sup>a</sup>Department of Physics, Vellore Institute of Technology, Vellore, Tamil Nadu, 632 014 India.

<sup>b</sup>Centre for Functional Materials, Vellore Institute of Technology, Vellore, Tamil Nadu, 632 014 India.

Received 19 April 2019; accepted 16 September 2021

Titanium doped Lithium Germanate ( $\text{Li}_4\text{TiGe}_2\text{O}_8$ ) is synthesized by ceramic double sintering route. Germanate is sintered at a temperature of  $900^\circ\text{C}$  for 30 min in a microwave furnace. The formation of glass was confirmed by the X-ray diffraction technique. Electric, dielectric, ferroelectric and piezoelectric properties are investigated. Dielectric studies performed from room temperature to  $500^\circ\text{C}$  showed a steady dielectric constant of approximately 75 throughout the investigated temperature. AC conductivity of the glass showed very high resistivity of the order of  $10^7\ \Omega\text{-cm}$ . Further, an ionic hopping conduction mechanism is suggested from the conductivity behaviour as a function of frequency. Ferroelectric hysteresis recorded at room temperature has exhibited a square loop suggesting very good ferroelectric nature of the glass. From the obtained high resistivity and piezoelectric coefficient, the glass can be explored for MMIC and MLCC device fabrication.

**Keywords:** Lithium titanium germanate, Dielectric constant, Ferroelectric, Piezoelectricity

### 1 Introduction

Lithium germanates are most widely used as a solid electrolyte in fuel cells, batteries, ion-selective membranes, charge storage devices etc and are studied for their ion transportation mechanism<sup>1,2</sup>. Sharonov *et al.*<sup>3</sup> has studied optical properties and emission spectra of  $\text{Cr}^{4+}$  doped lithium germanates for probable laser applications. However, lithium germanate is also doped with  $\text{Ti}^{4+}$  to study its non-linear optical behaviour and Mączka *et al.* and others<sup>4-6</sup> has reported ferroelastic phase transition nature at 233.5 K. Lithium titanogermanates reported so far are crystalline with layered structures<sup>1-7</sup>. These are extensively studied to develop a theoretical understanding of ferroelastic and co-elastic materials<sup>8,9</sup>. Various modified lithium germanates are studied mostly for their applications as ferroelastic, ferroelectric, optoelectronic, piezoelectric and photorefractive materials<sup>10</sup>. However, most of the investigations are focused on phase transformations, high resistivity at high temperatures and optoelectronic device applications<sup>11,12</sup>. But Lithium germanates are an important class of ferroelectric glasses that can be explored for their dielectric and ferroelectric device applications<sup>13</sup>. Further Titanium ( $\text{Ti}^{4+}$ ) is known for its high dielectric and ferroelectric nature in ceramics<sup>14</sup>. The low-temperature sintering of these glasses makes them more favourable for the development of monolithic

microwave integrated circuits (MMIC) and Multilayer ceramic capacitors (MLCC). In the present article, investigations of structure, electric, dielectric, ferroelectric and piezoelectric properties of titanium doped lithium germanate ( $\text{Li}_4\text{TiGe}_2\text{O}_8$ ) are reported.

### 2 Experimental Details

For the preparation of  $\text{Li}_4\text{TiGe}_2\text{O}_8$  (LTGO),  $\text{LiOH}\cdot\text{H}_2\text{O}$  (99% ; Sdfine),  $\text{TiO}_2$  (99.9% ; Alfa Aesar),  $\text{GeO}_2$  (99.999% ; Otto Chemicals) are used for the synthesis. All the chemicals are used as received. Stoichiometric amounts of the starting materials are weighed and hand grinded for 3 hours using agate mortar and pestle. The powders are pressed into cakes and calcined at  $430^\circ\text{C}$  for 30 min using a microwave furnace. The calcination accomplishes partial reaction for the final compound to form. Again Pellets are grinded for 4 hours using agate mortar and pestle. Green powders are made into pellets with a drop of polyvinyl alcohol by uniaxial pressing in a 1cm dye and sintered at  $900^\circ\text{C}$  for 30 min in a microwave furnace.

Structural properties of the sample are studied by powder X-ray diffraction technique using X-ray diffractometer (Bruker, D8 Advance) with  $\text{Cu K}\alpha$  radiation ( $\lambda = 1.54056\text{\AA}$ ). Pellets are painted with silver paste on both sides for good ohmic contact. Pellets are poled for 30 min at 1kV/cm to align the dipoles in the direction of the applied field. At  $30^\circ\text{C}$ ,

\*Corresponding author (E-mail: madhuriw12@gmail.com)

variation of polarization with applied electric field is measured using Marine India PE Loop Tracer. Thermal spectra of dielectric constant and loss tangent are estimated using LCR meter (LCR HiTESTER 3532-50-HIOKI). Piezoelectric voltage and  $d_{33}$  are measured using YE2730A  $d_{33}$  meter (SINOCERA piezotronics).

### 3 Results and Discussion

#### 3.1 Structural properties of LTGO

Fig. 1 provides the X-ray diffraction (XRD) profile of the powdered LTGO sample. The intensity of the diffracted X-ray data is plotted as a function of diffraction angle  $2\theta$ . The X-ray pattern suggests the formation of amorphous glass with partial secondary phases. The observed peaks could be best indexed to  $\text{Li}_4\text{GeO}_4$  phase and orthorhombic structure as reported in JCPDS file no. 72-1408. The observed peaks could be assigned to reflections from (101), (111), (020), and (311) Miller planes, for ascending  $2\theta$  values.

#### 3.2 Dielectric properties

The dielectric properties,  $\epsilon(\omega)$ , of the sample consists of a real component ( $\epsilon_r(\omega)$ ) which is known as dielectric constant and an imaginary component ( $\epsilon''(\omega)$ ) which is known as dielectric loss as shown in equation (1).

$$\epsilon(\omega) = \epsilon_r(\omega) + i \epsilon''(\omega) \quad \dots(1)$$

$$\epsilon_r = C_p / C_o \quad \dots(2)$$

The dielectric constant is calculated for 1 kHz, 10 kHz and 100 kHz frequencies at different temperatures

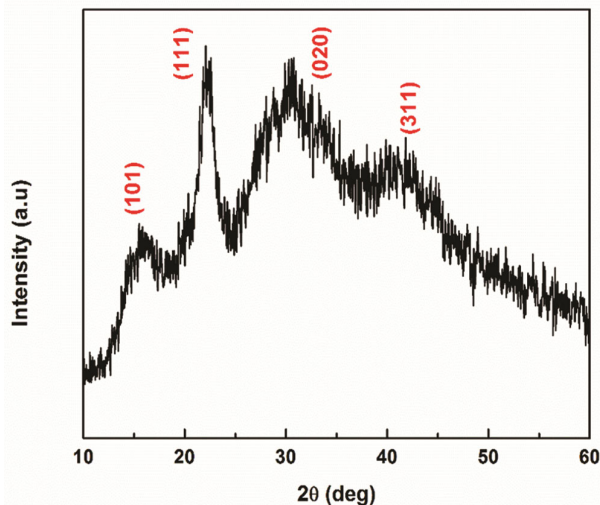


Fig.1 – X-ray diffraction profile of LTGO.

using equation (2). where  $C_p$  is the parallel capacitance and  $C_o$  is the geometric capacitance of the sample. Fig 2 shows the temperature dependence of the dielectric constant  $\epsilon_r(T)$  of LTGO at 1 kHz, 10 kHz and 100 kHz frequencies. A slight decrease of the dielectric constant is noticed at temperatures 130 °C and 300 °C for all the frequencies. These dips of  $\epsilon_r$  might be due to electrical fluctuations during the measurements or thermal stresses on the dipole moment. It is worthwhile to note here that the dielectric constant is steady throughout the temperature range studied. The steady dielectric constant in the wide temperature range is attributed to the use of microwave furnace for final sintering of the glass which yielded a good quality glass. Further, a steady dielectric constant in a broad temperature range makes it a potential candidate for high-temperature device applications. In the whole temperature range, the  $\epsilon_r$  decreases with an increase in the applied electrical field frequency. This is a general behaviour of dielectrics. As the dipoles do not respond for the higher frequencies, the  $\epsilon_r$  decreases with frequency.

Figure 3 shows the frequency dependent dielectric loss ( $\epsilon''$ ) of LTGO at different temperatures. At different temperatures,  $\epsilon''$  decreases with increase in the applied frequencies. Also,  $\epsilon''$  increases with increase in the temperature at the low frequencies. This means that at room temperature, the sample will show a very low loss factor. This kind of low loss material is suitable for devices that need noise suppression.

#### 3.3 AC electrical conductivity studies

AC conductivity ( $\sigma_{ac}$ ) is calculated using equation (3).

$$\sigma_{ac} = \frac{Gd}{A} \quad \dots(3)$$

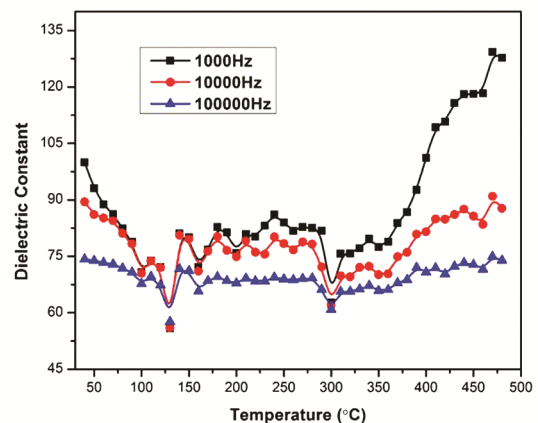


Fig. 2 – Temperature-dependent dielectric constant ( $\epsilon_r$ ) of LTGO at different frequencies.

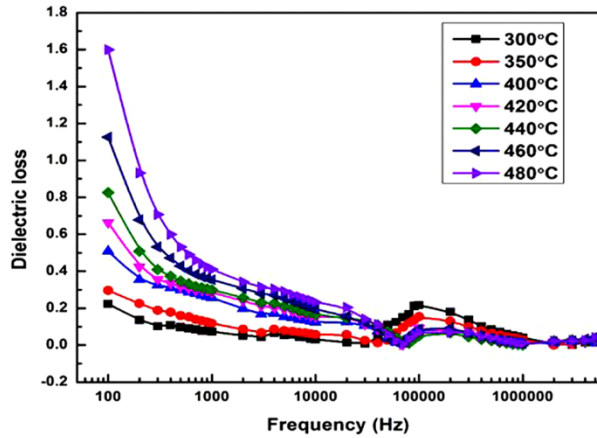


Fig. 3 – Frequency-dependent dielectric loss ( $\epsilon''$ ) of  $\text{Li}_4\text{TiGe}_2\text{O}_8$  at different temperatures.

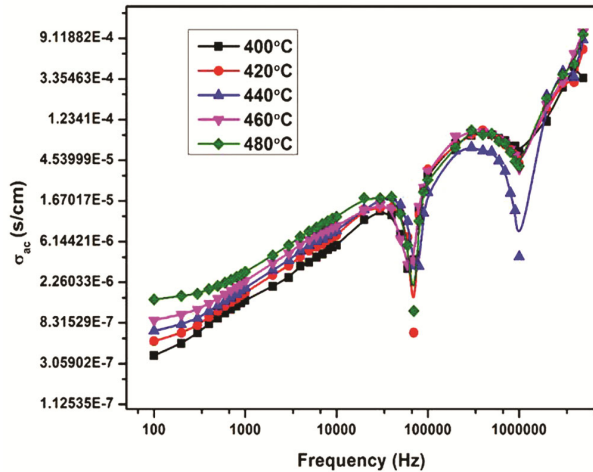


Fig. 4 – Frequency scan of AC conductivity of LTGO.

where  $G$  is the electrical conductance,  $d$  is the thickness and  $A$  is the area of the sample. Fig 4 shows the relationship between the ac electrical conductivity and frequency at different temperatures. The system exhibited high resistivity even at a high temperature of the order of  $10^7 \Omega\text{-cm}$  at around  $500^\circ\text{C}$ . The data shows that there is more dispersion at the low-frequency region compared to the high-frequency region. The  $\sigma_{ac}$  increases with an increase in frequency. The increase of  $\sigma_{ac}$  with frequency is due to the presence of various kinds of inhomogeneity present in the material. Lithium promotes ionic conductivity and lithium germinates exhibit ionic conduction<sup>14</sup>. As hopping of charge carriers is universal in oxide semiconductors, the ionic hopping conduction mechanism is predominant in the present system<sup>15</sup>. Further linear increase in conductivity strongly supports the hopping conduction mechanism. The troughs at 900 kHz and 1 MHz must be carry forwarded

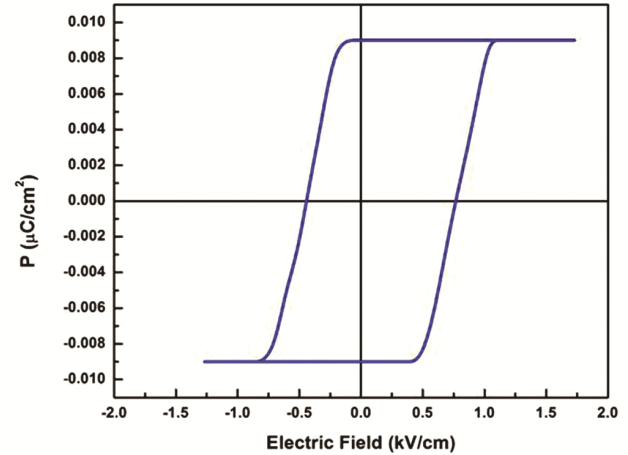


Fig. 5 – P-E loop for LTGO at room temperature.

from the dielectric studies and are assumed due to power supply fluctuations. The change in the slope of ac conductivity indicates the change in the hopping frequency of the carriers. However further analysis of ac conductivity may confirm the type of conduction.

#### 3.4 Ferroelectric and piezoelectric properties

The ferroelectric materials exhibit spontaneous polarization. The variation of dielectric polarisation as a function of the electric field results in a hysteresis loop (PE loop). It helps us to understand the ferroelectric property of the material. Fig 5 shows the P-E loop at room temperature with fixed resistance of  $1\text{M}\Omega$  and a capacitance of  $1\text{nF}$ . The coercivity and the remnance of the prepared sample LTGO is  $0.6 \text{ kV/cm}$  and  $9\text{pC/cm}^2$  respectively.

The piezoelectric coefficient ( $d_{33}$ ) is the induced polarization per unit applied stress. The piezoelectric voltage susceptibility ( $g_{33}$ ) is defined as the mechanical deformation of the piezoelectric material per unit potential developed.  $d_{33}$  value of LTGO is found to be  $96 \text{ pC/N}$  and the  $g_{33}$  is calculated using the equation (4).  $g_{33}$  value of LTGO is found to be  $783 \text{ fm/V}$ .

$$g_{33} = \frac{d_{33}}{\epsilon_{33}} \quad \dots (4)$$

where  $d_{33}$  is the piezoelectric coefficient and  $\epsilon_{33}$  is the dielectric constant of the sample at room temperature.

#### 4 Conclusions

$\text{Li}_4\text{TiGe}_2\text{O}_8$  glass dielectric is synthesized by a solid-state reaction route. The X-ray diffraction analysis revealed amorphous glass formation with partial  $\text{LiGeO}_4$  crystallization. The dielectric constant is found to be in the range of 75 and 100 and a low dielectric loss is observed at room temperature. A steady dielectric

constant in the investigated temperature range is attributed to the glass formation quality and use of microwaves for final sintering. A linear increase in the ac conductivity with applied frequency confirmed the ionic hopping conduction mechanism in the glass. The change in slope suggests the existence of different hopping frequencies of the carriers at these frequencies. Very high resistivity at elevated temperature and a good piezoelectric response is noticed at room temperature promising further modification of the composition may lead to high  $d_{33}$  piezoelectric material at low sintering temperatures useful for monolithic microwave integrated circuits (MMIC) and multilayer ceramic capacitor (MLCC) applications.

### Acknowledgements

The authors acknowledge the XRD facility at SAS, VIT, Vellore and are very much thankful to Prof. S. Kalainathan, VIT, Vellore for providing dielectric and ferroelectric measurement facilities.

### References

- 1 Kireev V V, Yakubovich O V, Ivanov-Shits A K, Mel'nikov O K, Dem'yanets L N, Skunman, J & Chaban N G, *Russ J Coordinat Chem*, 27 (2001) 31.
- 2 Liu Y, Bai Q, Nolan A M, Zhou Y, Wang Y, Mo Y & Xia Y, *Nano Energy*, 66 (2019) 104094.
- 3 Sharonov M Y, Bykov A B, Owen S, Petricevic V & Alfano R R, *J Appl Phys*, 93 (2003) 1044.
- 4 Mączka M, Sieradzki A, Poprawski R, Hermanowicz K & Hanuza J, *J Phys Condens Matter*, 18 (2006) 2137.
- 5 Przesławski J, Poprawski R, Just M, Kireev V V, Mielcarek S & Mróz, *Ferroelectrics*, 267 (2002) 201.
- 6 Poprawski R, Przesławski J, Kireev V V & Schaldin Y V, *Physica Status Solidi*, 9 (2001) 9.
- 7 Bastow T J, Botton G A, Etheridge J, Smith M E & Whit H J, *Acta Cryst*, 55 (1999) 2.
- 8 Sieradzki A, Cizman A, Strzęp A, Poprawski R, & Ryba-Rymanowski W, *Ferroelectrics*, 429 (2012) 56.
- 9 Sieradzki A, Pietraszko A & Poprawski R, *Integrated Ferroelectrics*, 62 (2004) 79.
- 10 Golubev N V, Sigaev V N, Stefanovich S Y, Honma T & Komatsu T, *J Non Cryst Solids*, 35417 (2008) 1909.
- 11 Blaszczyk K & Adamczyk A, *J Mol Struct*, 596 (2001) 61.
- 12 Sigaev V N, Lotarev S V, Orlova E V, Stefanovich S Y, Pernice P, Aronne A, Fanelli E & Gregora I, *J Non Cryst Solids*, 353 (2007) 1956.
- 13 Luo H, Fang L, Xiang H, Tang Y & Li C, *Ceram Int*, 43 (2017) 1622.
- 14 Liebert B E & Huggins R A, *Mater Res Bull*, 11 (1976) 533.
- 15 Puli V S, Orozco C, Picchini R & Ramana C V, *Mater Chem Phys*, 184 (2016) 82.